Supplementary information

Supplementary Text

Calcium is involved in diverse cellular functions. The presence of a calcium pump-like domain (209-264 a.a.) in the 3a protein indicates its influence on cellular calcium-related functions [4, 5]. A large chromosome deletion, *Df(3L)Exel6138*, which uncovers the 79D3-E3 region showed a strong dominant suppression of the *EGFP-3a*-induced rough eye phenotype (Supplementary Fig. 3C). The *Cysteine String Protein* (*Csp*) locus is located in the 79D3 region on the third chromosome; and *Csp* has been demonstrated to play modulatory roles on calcium channel function [41]. To confirm that the *Df(3L)Exel6138* modifying effect was due to loss-of-function of *Csp*, an imprecise excision allele of *Csp* (Csp^{R1}, [42]) was crossed to *EGFP-3a*, and a strong suppression of the rough eye phenotype was observed (Supplementary Fig. 3D). Further, a concomitant reduction of Csp protein level was observed in Csp^{R1} suppression (Supplementary Fig. 3E). Csp is an evolutionarily conserved protein, and the human Csp

protein is expressed in various tissues including the lung [43]. In addition to *Csp*, we also recovered *Calpain B* (a calcium activated protease) and *PAST1* (Putative Achaete Scute Target 1; an EH-hand calcium binding motif-containing protein) as *EGFP-3a* modifiers from our genetic screen (Table 1). These modifications further highlight the action of *3a* on cellular calcium functions.

References

[4] A. D. Singh, D. Gupta, and S. Jameel, Bioinformatic analysis of the SARS virus X1 protein shows it to be a calcium-binding protein., Curr. Sci. 86 (2004) 842-844.

[5] C. J. Yu, Y. C. Chen, C. H. Hsiao, T. C. Kuo, S. C. Chang, C. Y. Lu, W. C. Wei, C. H. Lee, L. M. Huang, M. F. Chang, H. N. Ho, and F. J. Lee, Identification of a novel protein 3a from severe acute respiratory syndrome coronavirus, FEBS Lett 565 (2004) 111-116.

[41] L. C. Miller, L. A. Swayne, J. G. Kay, Z. P. Feng, S. E. Jarvis, G. W. Zamponi, and J. E. Braun, Molecular determinants of cysteine string protein modulation of N-type calcium channels, J Cell Sci 116 (2003) 2967-2974.

[42] K. K. Eberle, K. E. Zinsmaier, S. Buchner, M. Gruhn, M. Jenni, C. Arnold, C. Leibold, D. Reisch, N. Walter, E. Hafen, A. Hofbauer, G. O. Pflugfelder, and E. Buchner, Wide distribution of the cysteine string proteins in Drosophila tissues revealed by targeted mutagenesis, Cell Tissue Res 294 (1998) 203-217.

[43] T. Coppola, and C. Gundersen, Widespread expression of human cysteine string proteins, FEBS Lett 391 (1996) 269-272.

Supplementary Fig. 1. Generation of SARS-CoV 3a monoclonal antibodies. (**A and B**) Western blot analysis of the anti-3a monoclonal antibodies. Two anti-3a IgG 1 monoclonal antibodies, MAb X61 and X98, were raised against a C-terminal 60-mer peptide (**A**). Immunoreactive bands (**B**) were detected by the monoclonal antibodies MAbs X61 and X98 in cell lysates prepared from CHO cells transiently transfected with a His-tagged full-length 3a construct (+). X103 which showed no anti-3a activity, and untransfected CHO cell lysates (-) were used as negative controls. (**C**) Immunofluorescence of 3a protein in SARS-CoV-infected Vero E6 cells. Punctate cytoplasmic localization pattern was observed in SARS-CoV-infected Vero cells stained with both MAbs X61 (2-5) and X98 (2'-5'). Uninfected Vero cells were used as negative control (1 and 1').

Supplementary Fig. 2. Genetic characterization of SARS-CoV *3a* gene in *Drosophila* eye. **(A and B**) Misexpression of the SARS-CoV *3a* gene disrupts the regular ommatidial structures in adult *Drosophila* eye. *gmr-GAL4* alone (**A**) showed normal external eye morphology, whereas flies misexpressed with the SARS-CoV *3a* transgene (**B**) resulted in a rough eye phenotype. (**C and D**) Subcellular localization of the 3a protein in *Drosophila*. Only background signals were observed in control (*34B-GAL4*) third instar salivary gland cells when stained with MAb X98 (**C**). A distinct punctate cytoplasmic pattern of the 3a protein was detected by MAb X98 when *3a* was misexpressed (**D**). (**E and F**) Misexpression of *3a* increases the number of apoptotic cells in third instar larval eye imaginal discs. Basal numbers of acridine orange-positive cells were observed in the control eye disc *(gmr-GAL4;* **E***)*. Expression of *3a* increased numbers of acridine orange-positive cells (**F**). Arrows indicate the location of the morphological furrows.

Supplementary Fig. 3. *Cysteine string protein* interacts genetically with *EGFP-3a* in the *Drosophila* eye. Misexpression of *EGFP-3a* caused a rough eye phenotype in adult flies (**B**). A large chromosome deletion *Df(3L)Exel6138* (**C**) and a gene-specific deletion Csp^{R1} **(D)** dominantly suppressed the *EGFP-3a*-induced rough eye phenotype. (**E**) Western blot analysis showed reduction of Csp protein levels in both deletion mutants.

Supplementary Figure 1

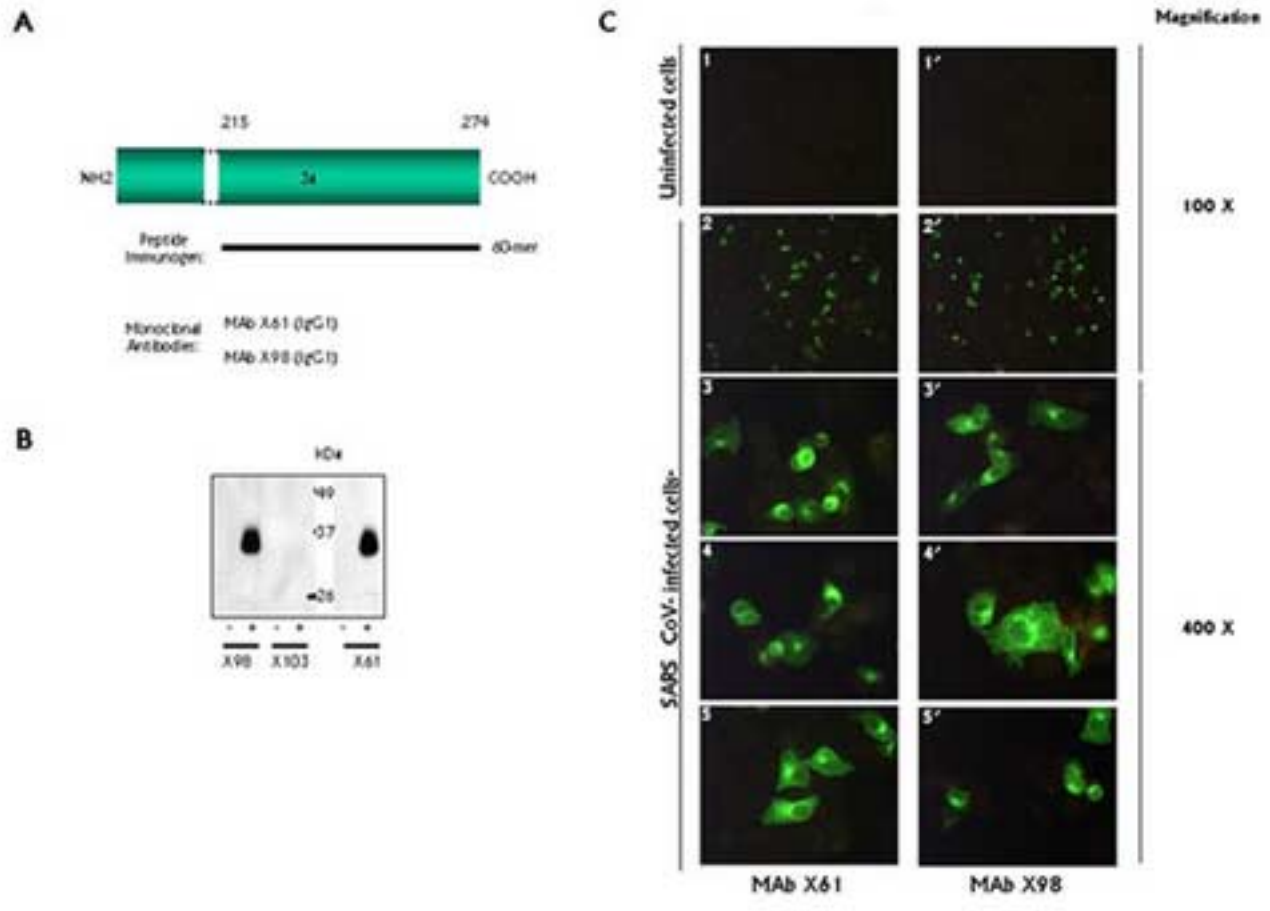

Supplementary Figure 2

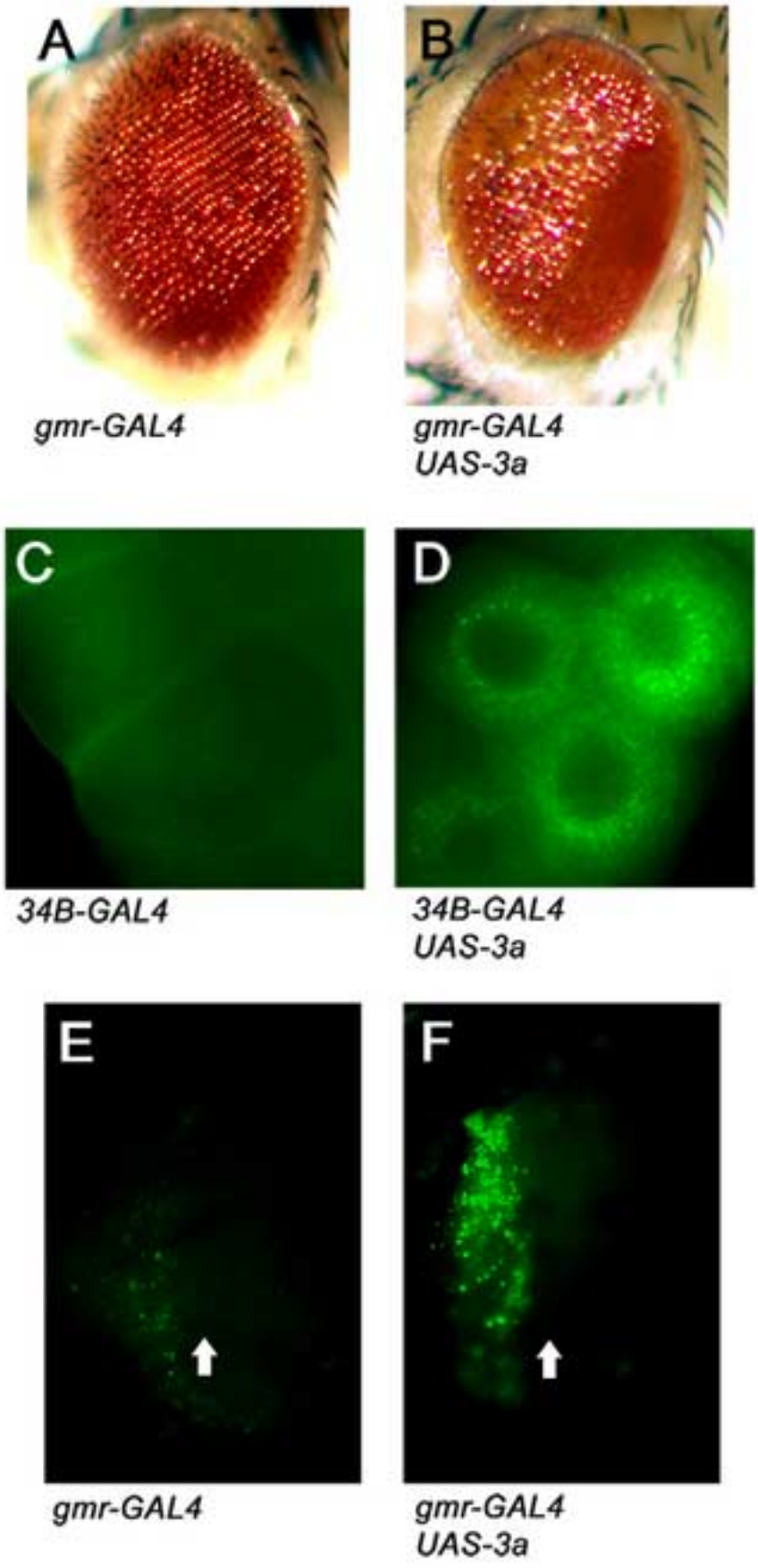

Supplementary Figure 3